

Behavior of Steel Intermediate Moment Frames Designed According to Iranian National Building Code under Lateral Load

H. Ramezansfat, A.A. Aghakouchak & S. Shahbeyk
Tarbiat Modares University, Tehran, Iran



SUMMARY

Intermediate moment frames are expected to withstand limited inelastic deformations in their members and connections when subjected to the lateral forces. The objective of this paper is to review the analysis and design criteria for Intermediate moment frames under lateral loads which have recently been added to the Iranian codes. So, two frames with 8 and 12 stories have been designed according to the Iranian codes. Then some samples of designed connections are modeled and analyzed in finite element software. Based on the calculations of the rotation capacity of the connections, a simplified model is developed. Then the model is employed for modeling and analysis of the frames. The results indicate that this type of connections can achieve 0.02 radian interstory drift angle without fracture. In addition the results of nonlinear static analysis of IMFs indicate that these frames satisfy the intended performance level when subjected to design earthquake.

Keywords: Intermediate moment frame, Moment-rotation curve, Performance level, nonlinear static analysis.

1- INTRODUCTION

Steel moment resisting frames (MRF) are assemblages of beams and columns, in which the beams are rigidly connected to the columns. Resistance to lateral force is provided primarily by the development of bending moments and shear forces in the frame members and joints. The bending rigidity and strength of the frame members is therefore the primary source of lateral stiffness and strength for the entire frame [Bruneau, 1997].

The moment frame connection included in the 1992 AISC seismic provisions [AISC, 1992] was based primarily on testing that was conducted in the early 1970s [popov and Stephen, 1972] indicating that a moment connection could accommodate inelastic rotations in the range of 0.01 to 0.015 radian. It was judged by engineers at the time that such rotations, which corresponded to building drifts in the range of 2 to 2.5 percent, were sufficient for adequate frame performance [AISC, 2005]. In the 1994 Northridge earthquake, unexpected brittle failures of MRFs were detected [SAC, 1994]. After this earthquake, many experimental tests and analytical studies were conducted on MRFs to investigate the causes of the brittle failures. The investigations emphasized that many changes that took place in materials, welding, frame configurations and member sizes since the 1970s make the original results unsuitable as a basis for design [AISC, 2005]. Additionally analyses using time histories, including P- Δ effects, demonstrate that drift demands may be larger than previously assumed [Krawinkler and Gupta, 1998]. Also the tests sought to provide reliable and economical solutions to the problems in MRFs [Kim 2000, Lee 1997, Engelhardt 1994, 1998, Han 2007]. As a result of such efforts, new seismic design criteria for steel moment frames [FEMA 350, 2000] were developed. AISC Seismic Provisions [AISC 1997, 2002, 2005] have also been significantly revised. For instance, the building code was amended to include substantial additional

requirements for special moment frames (SMF) system design and construction, resulting in an increase in the development cost for such structures. Therefore in 1997, the Intermediate moment frames (IMF) system was added to FEMA-302 and the AISC Seismic Provisions to provide an economical alternative to SMF construction for regions of moderate seismicity [FEMA 350, 2000].

Iranian Standard No.2800 and the Chapter ten of the Iranian National Building Codes have defined three types of seismic steel moment resisting frames similar to the AISC Seismic Provisions: Special moment frames, intermediate moment frames, and ordinary moment frames. Intermediate moment frames (IMFs) are expected to withstand limited inelastic deformations in their members and connections when subjected to the forces resulting from the ground motion of the design earthquake. Beam to column connections in IMFs are required to have a minimum inelastic rotation capacity of 0.02 radians. The objective of this paper is to review the analysis and design criteria for IM frames under lateral loads which have recently been added to the Iranian codes. Also as research on inelastic behaviors of this type of moment frame has not been conducted sufficiently; a simplified model is proposed to forecast this behavior.

2- CONNECTION MODELING

When a moment resisting frame is subjected only to lateral loading, it deforms as shown in Fig. 2.1. (a) and 2.1. (b). In this case, columns and beams between adjacent bays and stories are in double curvature. A change in the direction of flexure represents an inflection point, and therefore, a theoretical location of zero moment. This condition can be modeled by separation of the part of the frame within the inflection points and by applying boundary condition and loads that represent the internal stresses of the structure as seen in Fig. 2.1. (c). The strength and displacement capacities of the entire structure can be calculated as a combination of the performances of the individual sections.

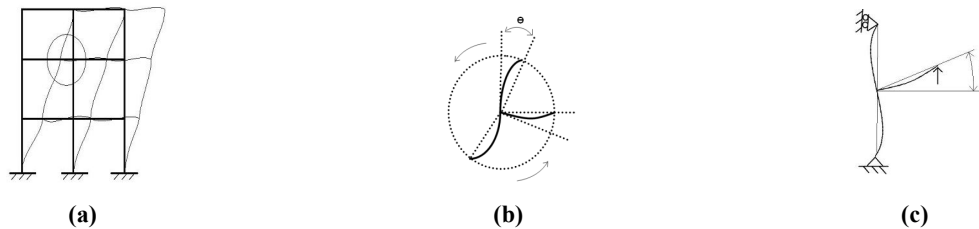


Figure 2.1. Isolation of Frame Section

This paper presents the results of a study of IMFs in buildings of two different heights (8 and 12-stories), which are located in a high seismic zone and are designed according to the Iranian National Building Codes. In this study, two connections are investigated in detail, connection H400 and H450, in which beam depth are equal to 400 mm and 450 mm respectively. In these connections columns are rectangular box sections of 350 x 350 mm. Connection of beam and columns are achieved through flange plates while the beam flanges are not welded to columns. Shear tabs are used to connect the beam webs to column. Internal continuity plates are installed to form a reliable shear panel in column section.

The connections are modeled in finite element software using three-dimensional brick elements, called SOLID45. This element is defined by eight nodes having three degrees of freedom at each node. This element has plasticity and large strain capabilities. The members in the model are assumed to be made of A36 steel and for weld metal, E60 electrodes are used. The true stress and true strain curves are used for modeling material behavior (Fig. 2.2., 2.3.). The effect of the material and geometric nonlinearities is accounted in the analysis of the model. For this purpose isotropic hardening is assumed.

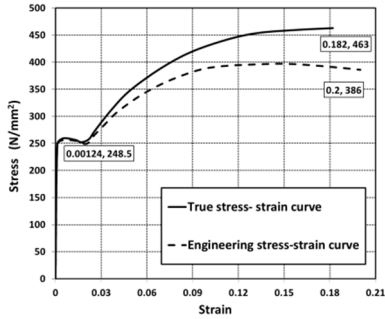


Figure 2.2. Stress-Strain Curve of steel.

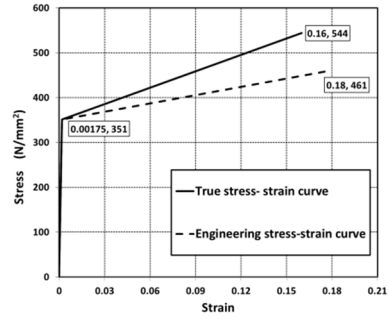


Figure 2.3. Stress-Strain Curve of weld Metal.

In order to study the nonlinear behavior of the subassembly consisting of half lengths of beam, columns and their connection, as shown in Fig 2.4., concentrated loading in terms of displacement is applied at the free end of the beam and is increased gradually to achieve a story drift of 0.02 radians. The bottom and top of the column has pinned end condition.



Figure 2.4. The connection subassembly was used in the finite element study.

3- DERIVATION OF MOMENT-ROTATION CURVE

Moment-rotation curve can be plotted for different regions of connection by using the data obtained from the analysis. The deformation of beam to column connection comprises of panel zone deformation (region 1 Fig. 3.1.), deformation of the region of the beam close to the column face (region 2 Fig. 3.1.) and plastic deformation which is concentrated at the distance d (beam depth) beyond the face of the column (region 3 Fig. 3.1.).

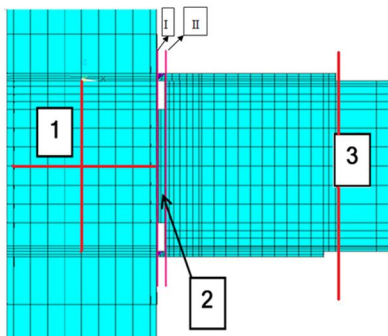


Figure 3.1. Different Regions of Beam to Columns Connection.

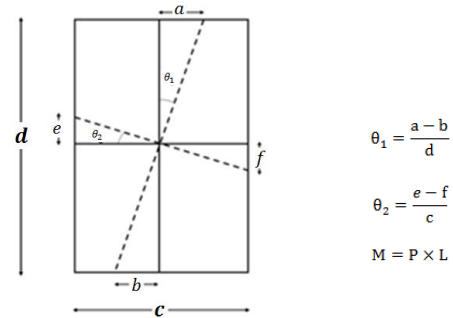
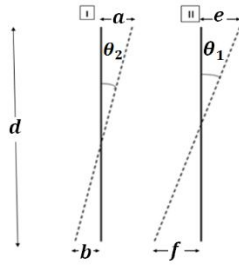
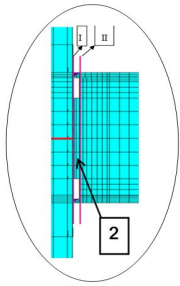


Figure 3.2. Calculation of θ in First Region.

The rotation angles of the first and second regions are computed according to the Fig. 3.2. and Fig. 3.3. by subtracting the rotations of selected lines ($\theta = \theta_1 - \theta_2$). In these figures, d is equal to beam depth and c is equal to column depth. The rotation angle of third region is computed according to the Fig. 3.4.



$$\theta_1 = \frac{e-f}{d}$$

$$\theta_2 = \frac{a-b}{d}$$

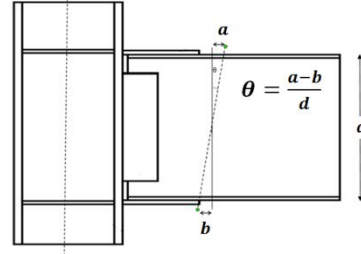


Figure 3.3. Calculation of θ in Second Region.

Figure 3.4. Calculation of θ in Third Region.

Comparison of moment rotation curves of these regions (Fig. 3.5. to 3.8.) reveals that inelastic deformation in beam plastic hinge region are significantly larger than the other regions. Fig. 3.5. shows that in these connections shear panels have behaved linearly. Also Fig. 3.6. shows that nonlinear behavior in second region is developed only when large amounts of moments are applied to the connection. But Fig. 3.7. and 3.8. show that at this level of applied moment, region 3 i.e. beam plastic hinge region has already undergone large inelastic deformations.

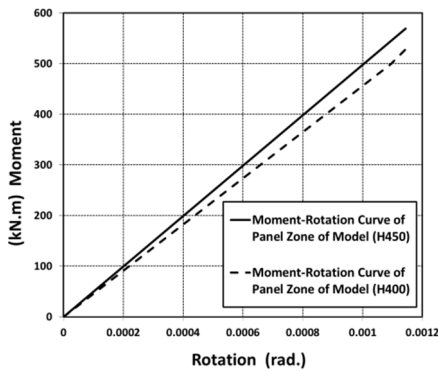


Figure 3.5. M- θ Curve of Panel Zone of Model H400, H450

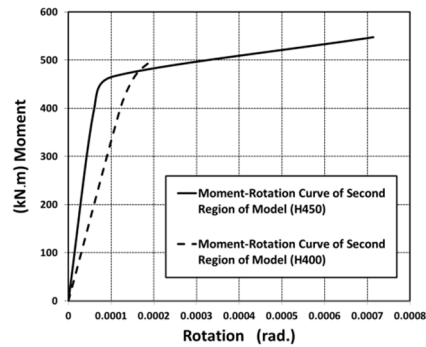


Figure 3.6. M- θ Curve of Second Region of Model H400, H450.

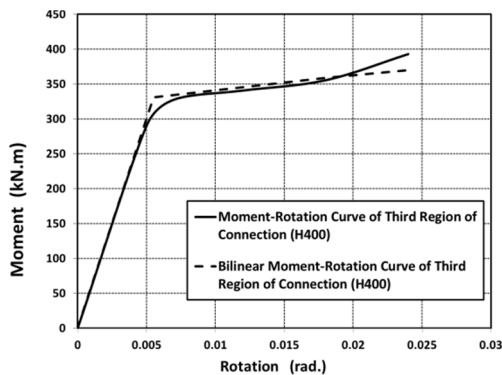


Figure 3.7. M- θ Curve of Third Region of Model H400.

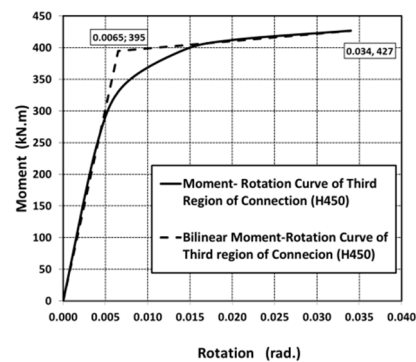


Figure 3.8. M- θ Curve of Third Region of Model H 450.

4- SIMPLIFIED MODEL

Detailed FE analysis of connections such as the one described in previous section is prohibitively time consuming if it is to be used for analysis of the entire frame. Hence the simplified model shown in Fig. 4.1 is developed by using the moment rotation curves obtained from the results of detailed finite element model. In this model, panel zone is modeled by a spring which acts as a scissor model (Castro 2005, Kim 2002, Krawinkler 1987). The (M- θ) curve of this region (Fig.3.5.) is considered for defining mechanical characteristics of this spring. A nonlinear rotational spring is used between the beam end and the column face to model the behavior of the second region of connection shown in Fig. 3.1. The (M- θ) curve obtained for this region (Fig. 3.6.) is considered for describing this spring. The plastic hinge behavior in the beam (Third region of Fig. 3.1.) is defined by the bilinear moment-rotation curves of Fig. 3.7.or 3.8. After creating the simplified model and performing a nonlinear static analysis, the force-displacement curves are compared with the result of detailed model (Fig. 4.2.). This comparison indicates that the simplified model produces results similar to the true behavior of the connection.

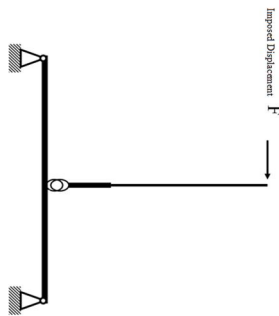


Figure 4.1. Simplified Model

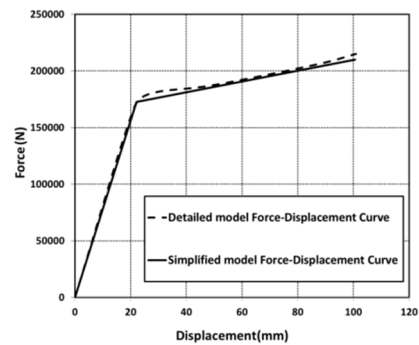


Figure 4.2. Comparison of Force-Displacement Curve of Connection obtained from simplified and detailed models

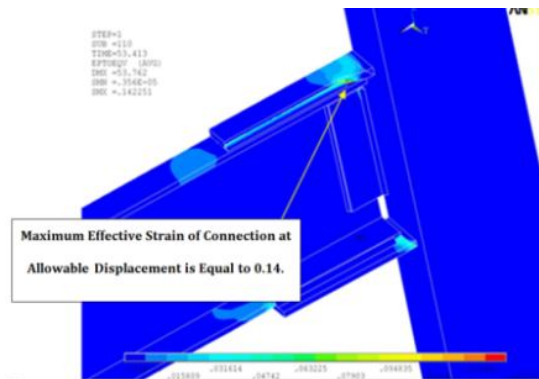


Figure 4.3. The Magnitude of Effective Strain of Connection H450 at Allowable Displacement.

The detailed model results also show that by applying 5 cm displacement at the end of the beam which is equal to 0.02 radian rotation, the maximum effective strain at the intersection of flange plate and column face is about 0.142 (Fig. 4.3.). This value is smaller than the ultimate strain in true stress-true strain curve of weld metal. Therefore without going to detailed investigation of cyclic behavior of the joint and assessing the damage that may cause connection failure, by using the simple criterion of maximum effective strain it may be concluded that this connection can sustain the applied rotation without any failure.

5. INVESTIGATING THE BEHAVIOR OF INTERMEDIATE MOMENT RESISTING FRAMES

Assessment of the overall performance of sample frames is presented in the following section. The frames under this investigation are 8- and 12 story ones for which two types of modeling is performed. In the first type of modeling of the frame, the simplified model of the connection shown in Figure 4.1 is used to model the connections. In this model plastic hinges in the beam are defined based on the bilinear $M-\theta$ curve which is obtained from detailed FE analysis (Fig. 3.7 & 3.8). In the second type of modeling of frames, elastic and inelastic deformations of beams, columns, connections and panel zones are defined according to the deformations limits of Table 5-6 of FEMA 356 [FEMA356, 2000]. Nonlinear static analysis of both models of the frames is carried out based on this code of practice.

5.1. Nonlinear Behavior of Components

5.1.1. Nonlinear behavior of connection and panel zone

Panel zone is modeled in both models. In the first model, characteristics of the spring representing the panel zone is obtained from detailed FE analysis, but in the second model, the spring specification is obtained from Table 5-6 of FEMA 356.

5.1.2. Nonlinear behavior of columns

In the first and second type of modeling, column elements are considered linear and their inelastic deformations, if any, are envisaged at plastic hinge locations considered at the ends of columns.

5.1.3. Nonlinear behavior of beams

Plastic hinge definition in the beams for the first type of modeling is based on the bilinear $M-\theta$ curve, which is obtained from detailed FE analysis. Hinge definitions in the second type of modeling are according to the Table 5-6 of FEMA 356.

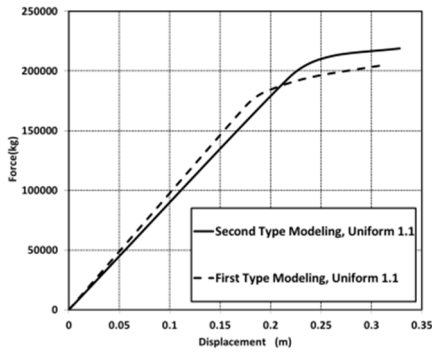
5.2. Deformations of Frames and Their Components

In order to assess the frames behavior, the diagram of base shear versus roof displacement is derived (Fig. 5.1. & 5.4.). Comparison of these curves indicates that before formation of plastic hinge, the slopes of these curves are approximately equal because the dimensions of the members, which have direct effect on the frames stiffness, are almost the same in both types of frame modeling. However because the panel zone stiffness in first model is larger than the second type frames, there is a negligible difference in frame stiffness. The main differences of responses of these two types of model appear after the formation of plastic hinge. Because the beams yield moment in the second type of frame are larger than the first type, they yield later and therefore the second type model has larger global yield shear strength (V_y) than the first type.

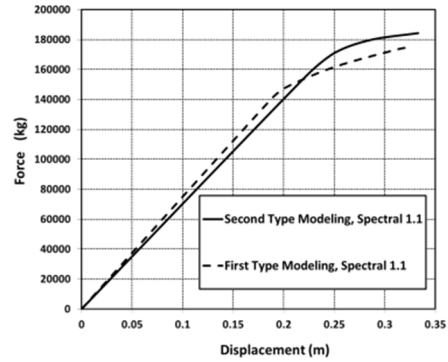
Fig. 5.2., 5.3., 5.5. and 5.6. show the deformed shapes of these frames when target displacement occur at roof level. Plastic hinges in blue indicate life safety level and the ones in pink indicate immediate occupancy performance level. The values of inelastic deformations indicate that the plastic hinges do not exceed the life safety levels. Therefore frames which are designed in accordance with Iranian Standard No.2800 and the Chapter tenth of the Iranian National Building Codes satisfy the intended performance level. Also because the beams yield moment in first type frames are smaller than the second type frames, therefore in these frames greater number of plastic hinge is observed.

Comparison of interstory drift of 8- and 12 story frames shows that in the nonlinear range, first model experienced larger interstory drift than the second model (Fig. 5.7.). Also this type of connections can achieve 0.02 radian inter story drift angle and satisfy the code criteria.

Tables 5.1. and 5.2 show the rotations of connections in two models of the frames under this study. They reveal that rotation of connection and panel zone in second type models are larger than similar values in first type models. However, panel zone and connections Performance Levels are Immediate Occupancy. So it can be concluded that when the connections and panel zone are designed based on the Iranian Standard No.2800 and the Chapter tenth of the Iranian National Building Codes, they will experience limited nonlinear behavior and plastic deformation will concentrate in beams albeit some nonlinearities also occur in columns.

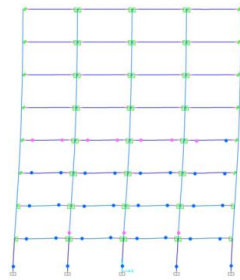


Lateral Loading: Uniform ,Gravity Load: 1.1 (D+L)

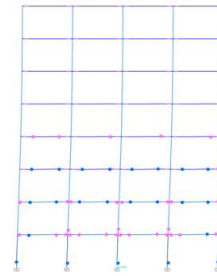


Lateral Loading: Spectral ,Gravity Load: 1.1 (D+L)

Figure 5.1. Base Shear-Roof Displacement Curve of First and Second Type Modeling of 8 Story Frame.

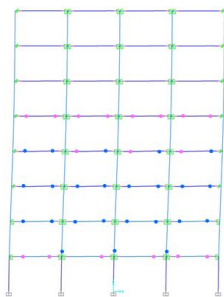


First Type Modeling

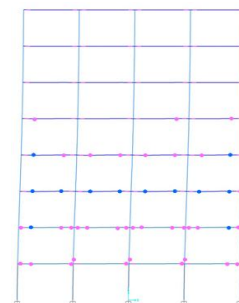


Second Type Modeling

Figure 5.2. Deformed shape of 8 story frame; Lateral Loading Type: Uniform, Gravity Load Type: 1.1 (D+L).

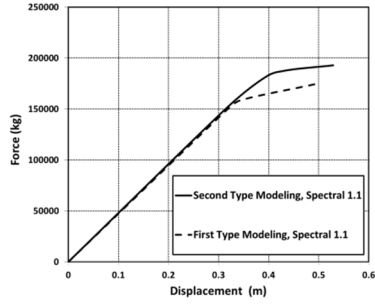


First Type Modeling

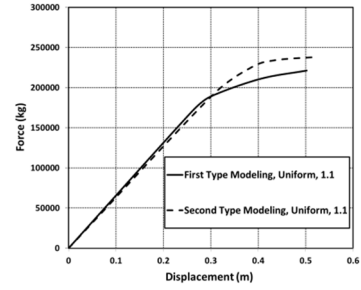


Second Type Modeling

Figure 5.3. Deformed shape of 8 story frame; Lateral Loading Type: Spectral, Gravity Load Type: 1.1 (D+L).

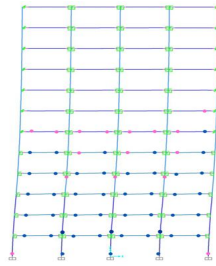


Lateral Loading: Spectral, Gravity Load: 1.1 (D+L).

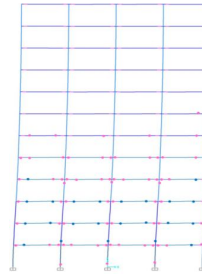


Lateral Loading: Uniform, Gravity Load: 1.1 (D+L).

Figure 5.4. Base Shear-Roof Displacement Curve of First and Second Type Modeling of 12 Story Frame.

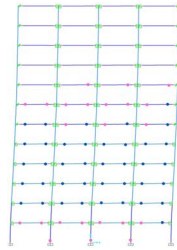


First Type Modeling.

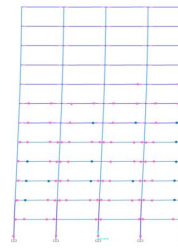


Second Type Modeling.

Figure 5.5. Deformed shape of 12 story frame; Lateral Loading Type: Uniform, Gravity Load Type: 1.1 (D+L).

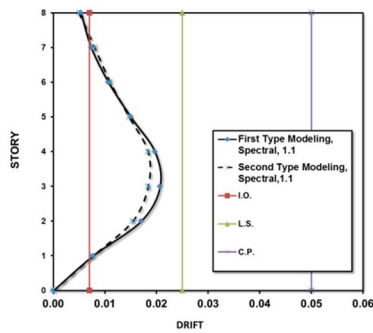


First Type Modeling.

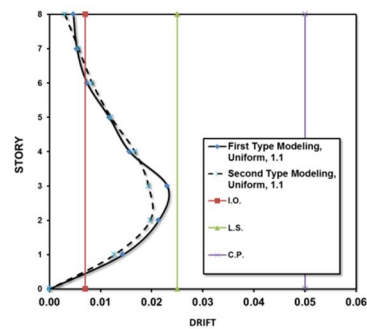


Second Type Modeling.

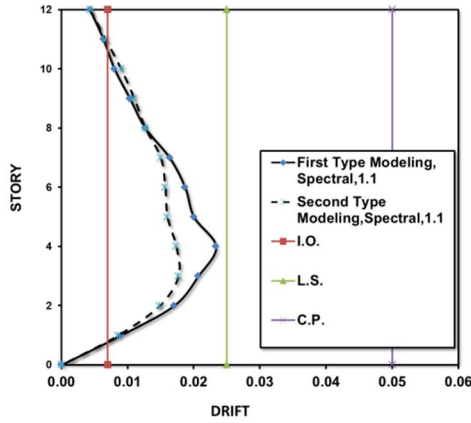
Figure 5.6. Deformed shape of 12 story frame; Lateral Loading Type: Spectral, Gravity Load Type: 1.1 (D+L).



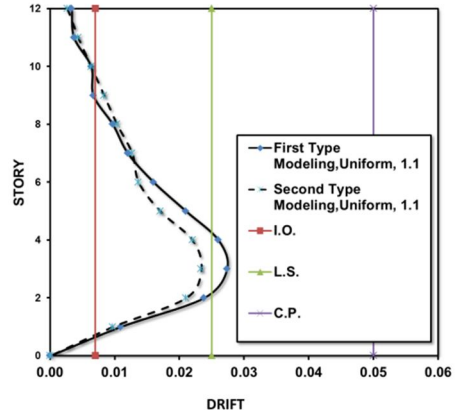
Lateral Loading: Spectral, Gravity Load: 1/1 (D+L).



Lateral Loading: Uniform, Gravity Load: 1/1 (D+L).



Lateral Loading: Spectral, Gravity Load : 1/1 (D+L).



Lateral Loading: Uniform, Gravity Load: 1/1 (D+L).

Figure 5.7. Comparison of Drift of First and Second Type Modeling of 8, 12 Story Frames.

Table 5.1. Performance Level of Connections of 8, 12 story frames.

First Type Modeling					Second Type Modeling						
MODEL	FLOOR	Spectral		Uniform		MODEL	FLOOR	Spectral		Uniform	
		θ_p		θ_p				θ_p		θ_p	
12 STORY	1	0.0001	B-I.O	0.0001	B-I.O	12 STORY	1	0.00053	B-I.O	0.0006	B-I.O
	2	0.00015	B-I.O	0.00016	B-I.O		2	0.00064	B-I.O	0.00082	B-I.O
	3	0.00015	B-I.O	0.00016	B-I.O		3	0.00068	B-I.O	0.00083	B-I.O
	4	0.00015	B-I.O	0.00016	B-I.O		4	0.00064	B-I.O	0.0007	B-I.O
	5	0.00012	B-I.O	0.00013	B-I.O		5	0.0006	B-I.O	0.00055	B-I.O
	6	-	A-B	-	A-B		6	-	A-B	-	A-B
	7	-	A-B	-	A-B		7	-	A-B	-	A-B
	8	-	A-B	-	A-B		8	-	A-B	-	A-B
	9	-	A-B	-	A-B		9	-	A-B	-	A-B
	10	-	A-B	-	A-B		10	-	A-B	-	A-B
	11	-	A-B	-	A-B		11	-	A-B	-	A-B
	12	-	A-B	-	A-B		12	-	A-B	-	A-B
8 STORY	1	0.00005	B-I.O	0.00008	B-I.O	8 STORY	1	0.00046	B-I.O	0.0006	B-I.O
	2	0.00008	B-I.O	0.0001	B-I.O		2	0.00067	B-I.O	0.0007	B-I.O
	3	-	A-B	-	A-B		3	0.000035	B-I.O	0.000014	B-I.O
	4	-	A-B	-	A-B		4	-	A-B	-	A-B
	5	-	A-B	-	A-B		5	-	A-B	-	A-B
	6	-	A-B	-	A-B		6	-	A-B	-	A-B
	7	-	A-B	-	A-B		7	-	A-B	-	A-B
	8	-	A-B	-	A-B		8	-	A-B	-	A-B

Table 5.2. Performance Level of Panel Zone of 8, 12 Story frames.

First Type Modeling					Second Type Modeling						
MODEL	FLOOR	Spectral		Uniform		MODEL	FLOOR	Spectral		Uniform	
		$\max(\frac{\theta_p}{\theta_{p,c}})$		$\max(\frac{\theta_p}{\theta_{p,c}})$				$\max(\frac{\theta_p}{\theta_{p,c}})$		$\max(\frac{\theta_p}{\theta_{p,c}})$	
12 STORY	1	-	A-B	-	A-B	12 STORY	1	0.5	B-I.O	0.7	B-I.O
	2	-	A-B	-	A-B		2	0.7	B-I.O	0.75	B-I.O
	3	-	A-B	-	A-B		3	0.7	B-I.O	0.75	B-I.O
	4	-	A-B	-	A-B		4	0.69	B-I.O	0.7	B-I.O
	5	-	A-B	-	A-B		5	0.68	B-I.O	0.68	B-I.O
	6	-	A-B	-	A-B		6	0.5	B-I.O	0.4	B-I.O
	7	-	A-B	-	A-B		7	0.45	B-I.O	0.2	B-I.O
	8	-	A-B	-	A-B		8	0.3	B-I.O	0.15	B-I.O
	9	-	A-B	-	A-B		9	0.15	B-I.O	-	A-B
	10	-	A-B	-	A-B		10	-	A-B	-	A-B
	11	-	A-B	-	A-B		11	-	A-B	-	A-B
	12	-	A-B	-	A-B		12	-	A-B	-	A-B
8 STORY	1	-	A-B	-	A-B	8 STORY	1	0.8	B-I.O	0.85	B-I.O
	2	-	A-B	-	A-B		2	0.8	B-I.O	0.9	B-I.O
	3	-	A-B	-	A-B		3	0.65	B-I.O	0.63	B-I.O
	4	-	A-B	-	A-B		4	0.60	B-I.O	0.50	B-I.O
	5	-	A-B	-	A-B		5	0.30	B-I.O	0.30	B-I.O
	6	-	A-B	-	A-B		6	-	A-B	-	A-B
	7	-	A-B	-	A-B		7	-	A-B	-	A-B
	8	-	A-B	-	A-B		8	-	A-B	-	A-B

6. CONCLUSION

The results of this study indicate that intermediate moment frames designed based on the Iranian Standard No.2800 and the Chapter tenth of the Iranian National Building Codes can achieve 0.02 radian inter story drift angle without exceeding the maximum tolerable strain. When these frames are subjected to lateral loads, inelastic deformations will be concentrated in a plastic hinge region which is located at the end of the flange plates in beam span. In this region, beam yielding starts at extreme fibers and then develops in cross section depth, therefore large strains occur at a distance away from the column face in parent material which is desirable.

Investigations show that the beams and columns of these frames are in life safety performance level when subjected to design earthquake. Therefore they satisfy intended performance level. Inelastic deformations of connections are limited and their performance can be categorized as immediate occupancy. Two types of modeling have been utilized in this study. Although larger inelastic deformations are observed in the first model, nevertheless the performance levels are the nearly the same for both models. Thus second type of modeling, which is according to the FEMA 356 recommendations and does not require detailed analysis of this type of connections, is appropriate for assessing the behavior of this type of frame.

REFERENCES

- AISC. (1992, 1997, 2002, 2005), Seismic Provisions for Structural Steel Buildings, Chicago (IL), American Institute of Steel Construction.
- Bruneau, M., Uang, C.M. and Whittaker, A. (1997), Ductile Design of Steel Structure, New York, McGraw Hill.
- Castro, J.M., Elghazouli, A.Y. and Izzuddin, B.A. (2005). Modeling of the panel zones in steel and composite moment frames, *Engineering Structure* **27**, 129-144.
- Engelhardt, M.D. and Sabol, T.A. (1994). Testing of Welded Steel Moment Connection in Response to The Northridge Earthquake, Northridge Steel Update I. American Institute of Steel Construction.
- Engelhardt, M.D. and Sabol, T.A. (1998). Reinforcing of steel moment connection with cover plates: benefit and limitation, *Engineering Structures* **20**.
- Engelhardt, M.D., Winneberger, T., Zekany, A.J. and Potyraj, T.J. (1998). Experimental investigation of dog bone moment connections, *Engineering. Journal of AISC*, 128-138.
- FEMA 302. (1997). NEHRP Recommended Provisions for Seismic Regulations for New Buildings and Other Structures, Part 1 - Provisions, prepared by the Building Seismic Safety Council for the Federal Emergency Management Agency, Washington, D.C.
- FEMA 350. (2000). Recommended Seismic Design Criteria for New Steel Moment Frame Buildings: FEMA 350, Richmond (CA): SAC Joint Venture.
- FEMA 356. (2000). Prestandard And Commentary For The Seismic Rehabilitation of Buildings ,Prepared by American Society of civil Engineers, Washington, D.C.
- Kim, K.D., Engelhardt, M. (2002). Monotonic and cyclic loading models for panel zones in steel moment frames. *Journal of Constructional Steel Research* **58**, 605-635.
- Kim, T., Whittaker, A., Gilani, A., Bertero, V. and Takhirov, S. (2000), Cover Plate and Flange Plate Reinforced Steel Moment Resisting Connections, Pacific Earthquake Engineering Research Center, Peer Report.
- Krawinkler, H. and Gupta, A. (1998). Story Drift Demand for Steel Moment Frame Structure in Different Seismic Region. *Proceeding of the 6th U.S. National Conference on Earthquake Engineering*. Seattle, WA.
- Krawinkler, H. and Mohasseb, S. (1987) Effects of Panel Zones Deformation on Seismic Response. *Journal of Constructional Steel Research*, **8**, 233-250.
- Lee, Ch., Uang, C.M. (1997). Analytical modeling and seismic design of steel moment connections with welded straight haunch. *Journal of Structural Engineering* **127**,1028-1035.
- Popov, E.P., Stephen, R.M. (1972). Cyclic loading of full-size steel connection. *American Iron and Steel Institute. Bulletin NO.21*. Washington D.C.
- SAC. (1995), Analytical and Field Investigations of Buildings Affected by The Northridge Earthquake of January 17, Rep. No. SAC-95/04, Richmond (CA), SAC Joint Venture.
- S.W. Han, G.U. Kwon and K.H. Moon, (2007). Cyclic behaviour of post-Northridge WUF-B connections. *Journal of Constructional Steel Research*, **63:3** ,365–374.